Original Article

PMP

Progress in Medical Physics 32(4), December 2021
https://doi.org/10.14316/pmp.2021.32.4.99
eISSN 2508-4453

Dosimetric Study Using Patient-Specific Three-Dimensional-Printed Head Phantom with Polymer Gel in Radiation Therapy

Yona Choi[1,2], Kook Jin Chun[2], Eun San Kim[2], Young Jae Jang[1,2], Ji-Ae Park[3], Kum Bae Kim[1], Geun Hee Kim[4], Sang Hyoun Choi[1]

[1]Research Team of Radiological Physics & Engineering, Korea Institute of Radiological and Medical Science, Seoul, [2]Department of Accelerator Science, Korea University, Sejong, Divisions of [3]Applied RI and [4]Applied Radiation Bioscience, Korea Institute of Radiological and Medical Science, Seoul, Korea

Received 31 August 2021
Revised 7 December 2021
Accepted 7 December 2021

Corresponding author
Sang Hyoun Choi
(shchoi@kirams.re.kr)
Tel: 82-2-970-1590
Fax: 82-2-970-1590

Purpose: In this study, we aimed to manufacture a patient-specific gel phantom combining three-dimensional (3D) printing and polymer gel and evaluate the radiation dose and dose profile using gel dosimetry.

Methods: The patient-specific head phantom was manufactured based on the patient's computed tomography (CT) scan data to create an anatomically replicated phantom; this was then produced using a ColorJet 3D printer. A 3D polymer gel dosimeter called RTgel-100 is contained inside the 3D printing head phantom, and irradiation was performed using a 6 MV LINAC (Varian Clinac) X-ray beam, a linear accelerator for treatment. The irradiated phantom was scanned using magnetic resonance imaging (Siemens) with a magnetic field of 3 Tesla (3T) of the Korea Institute of Nuclear Medicine, and then compared the irradiated head phantom with the dose calculated by the patient's treatment planning system (TPS).

Results: The comparison between the Hounsfield unit (HU) values of the CT image of the patient and those of the phantom revealed that they were almost similar. The electron density value of the patient's bone and brain was 996±167 HU and 58±15 HU, respectively, and that of the head phantom bone and brain material was 986±25 HU and 45±17 HU, respectively. The comparison of the data of TPS and 3D gel revealed that the difference in gamma index was 2%/2 mm and the passing rate was within 95%.

Conclusions: 3D printing allows us to manufacture variable density phantoms for patient-specific dosimetric quality assurance (DQA), develop a customized body phantom of the patient in the future, and perform a patient-specific dosimetry with film, ion chamber, gel, and so on.

Keywords: Polymer gel, Computed tomography, Magnetic resonance imaging, Treatment planning system, 3D printing

Introduction

Recently, high-precision and high-dose radiation therapy techniques, such as intensity-modulated radiation therapy (IMRT), stereotactic body radiation therapy (SBRT), and stereotactic radiosurgery (SRS), have been widely used in the field of radiation therapy [1-4]. Such therapies have the advantage of increasing the therapeutic effect by irradiating sufficient radiation to the lesion to be treated while maximizing protection by minimizing the radiation dose to nor-

mal tissues; however, they require high precision and accuracy. Patient-specific dosimetric quality assurance (DQA) measurements are always performed to verify that radiation is accurately irradiated based on the patient treatment plan to guarantee the accuracy of such treatment. Here, patient-specific DQA is conducted using a solid detector such as a slit-type PMMA phantom, ionization chamber, film, or glass dosimeter or using an array-type detector and phantom composed of a single material into which the detector can be inserted [5-8]. A patient treatment plan follows a three-dimensional (3D) dose distribution because it is conducted in three dimensions, whereas the commonly used method is limited to evaluating a fragmentary dose distribution by measuring a one- (1D) or two-dimensional (2D) dose distribution. In this current research, we performed 3D dose evaluations by arranging several liquid scintillators and radiochromic films. However, an accurate evaluation remains restricted because liquid scintillators (besides those using gamma rays) have disadvantages such as low efficiency, long decay time, and reduced energy resolution, and films have limitations due to the air gaps and errors introduced when stacking multiple sheets [9,10]. The dose of each patient is evaluated using a single-material phantom fabricated with a material that is equivalent to water since the phantom cannot consider the density and shape of the tissue of each patient. There are only a limited number of studies that have focused on accurately verifying a high-precision radiation treatment plan because patient-specific DQA is limited to converting a 3D dose distribution into a 1D and 2D dose distribution and drawing a comparison. Thus far, various studies have been conducted to overcome these challenges and accurately validate the patient treatment plan. Silveira et al. [11] confirmed the actual patient treatment dose and applicability of the polymer gel. However, they could not perform dose verification as that using a human body because they employed a cylindrical phantom composed of a single material. Lee et al. [12] performed a 3D dosimetry with the polymer-gel located inside the insert of a liver cancer model made with a 3D printer during SBRT treatment; they were unable to conduct a dose evaluation in the environment that resembles the insides of the human body since only the liver was printed in 3D and inserted into a single-material phantom. Matrosic et al. [13] evaluated a 3D dose distribution by irradiating a therapeutic dose to a phantom coated with a polymer gel; this was conducted using a commercially available plastic phantom and not a material that mimics the human body.

For a more accurate dose evaluation, a phantom should be manufactured with the same shape as the human body instead of using a uniform shape. A phantom can be created to represent the same shape of the different organs and bone densities of the patient using 3D printing technology. Then, the dose distribution can be evaluated using 3D printed phantom. A patient-specific phantom can be manufactured using precise images, such as magnetic resonance imaging (MRI), computed tomography (CT), and positron emission tomography/computed tomography (PET/CT) images, with materials that have a density similar to that of the human body for considering the characteristics of each patient. Furthermore, the effectiveness of the precision treatment can be verified through the treatment planning system (TPS) for actual patient treatment and for performing a 3D gel dosimetry using a customized phantom [14,15].

In this study, a patient-customized phantom was manufactured using polymer gel and CT images to measure the 3D dose distribution. The usefulness of the 3D-printed gel-based patient-customized phantom was verified through a comparative evaluation with the actual 3D dose of the treated patient.

Materials and Methods

1. Producing the gel phantom with 3D printing

For this study, a head phantom was manufactured by RTsafe (RTsafe, Athens, Greece) using the CT images of the patient to produce a patient-customized phantom [13]. The phantom produced by RTsafe uses a ColorJet printing technique from Project 360 3D Printer (3D Systems, Morrisville, NC, USA). After spraying the liquefied material layer by layer, the material is solidified using a high-performance ultraviolet (UV) light to create the shape of the phantom. Each phantom layer printed is 0.1 mm thick, and the phantom can be manufactured based on the patient's anatomy using the CT images. The 3D-printed head phantom comprises skin and bone structures, and the soft tissue is filled with a

polymer gel, which is a water-equivalent material that enables a 3D dose evaluation (Fig. 1).

2. Patient-specific dosimetric quality assurance

The CT images are captured to apply the patient-specific phantom to the patient-specific DQA. The tube voltage and current are considered under the same conditions as the CT image of the patient. Here, the slice thickness is set to 2.5 mm. The acquired CT image is then sent to Eclipse, which is a TPS. The rigid body image registration is conducted with the actual patient image. Then, this image and the Hounsfield unit (HU) are compared to evaluate the similarity. The treatment technology and dose irradiated to the patient are applied like in an actual setting to evaluate the usefulness of the manufactured phantom and gel dose evaluation in an actual treatment environment. To this end, the produced phantom was laid on the treatment table of Clinic iX (Varian Medical Systems, Palo Alto, CA, USA), the cone beam computed tomography (CBCT) was taken, and the setup was conducted using actual patient images. Then, IMRT was applied, and the energy was calculated as 6 MV. The CT image of the patient and the one from the 3D-printed phantom are shown in Fig. 2.

3. Polymer gel dosimetry

The irradiated phantom is analyzed through MRI scans,

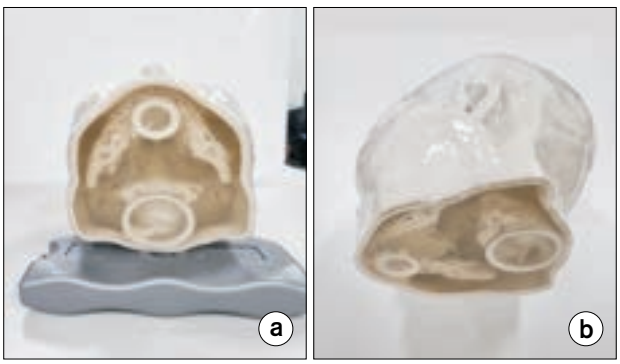

Fig. 1. (a, b) Manufacture of head phantom filled with a polymer gel.

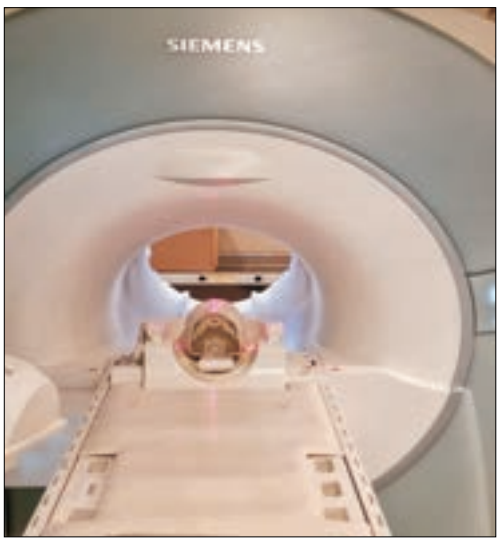

Fig. 3. Position alignment for magnetic resonance imaging (MRI) scans. Gel phantom scan image of the patient using MRI.

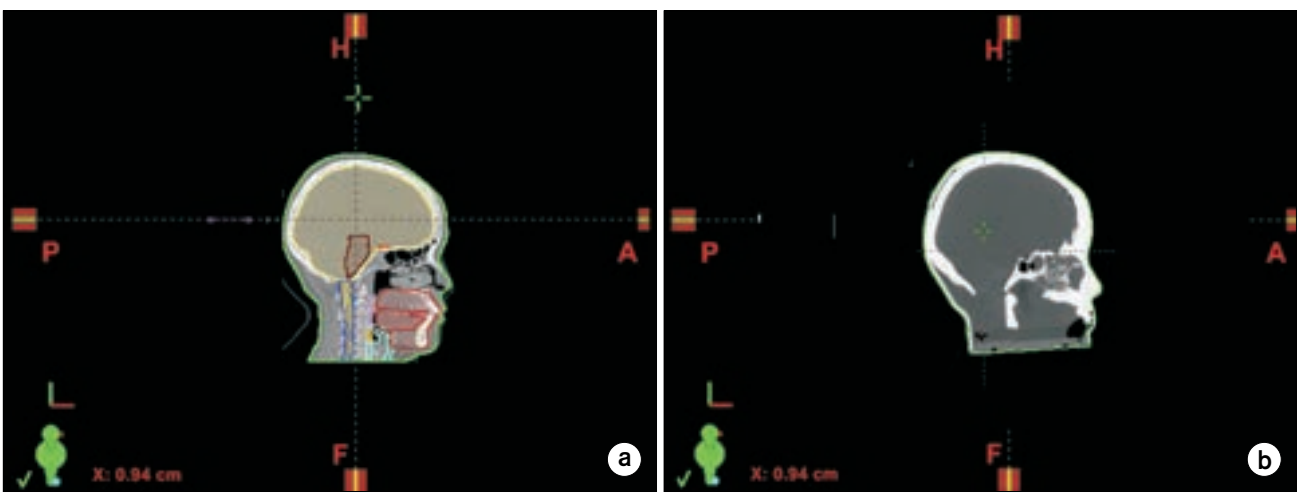

Fig. 2. (a) Computed tomography (CT) scan of the actual patient. (b) CT scan of the three-dimensional-printed head phantom.

and at least 5 hours of post-irradiation is required. Therefore, MRI scans are performed after 24 hours of post-irradiation. Fig. 3 shows the shape of the phantom scanned via MRI. For the optimal conditions of the phantom, the room temperature was maintained at 20°C to 24°C, and the MRI image was captured using Siemens MRI (Siemens Medical Solutions USA, Inc., Knoxville, TN, USA) with a magnetic field of 3 Tesla (3T). The total scan time of the phantom was 35 minutes 58 seconds, and the voxel size was 1.4×1.4×2.0 mm^3. 2D T2-weighted (T2-w) imaging was used, and images with 77 slices (slice thickness=2 mm, flip angle=180°, field of view (FOV)=350 mm, four constant times to echo (TEs) of 4.54 ms, and receiver bandwidth=781 Hz/Px) were acquired. The four TE/TRs measured over 2,000 ms of time repetition (TR) were TE[1]/TR 36/2,000 ms, TE[2]/TR 436/2,000 ms, TE[3]/TR 835/2,000 ms, and TE[4]/TR 1,230/2,000 ms. After scanning, the dose irradiated to the 3D polymer gel was analyzed using the MRI data as a 3D distribution. The detailed conditions are presented in Table 1.

Results

1. Head phantom

The electron density value of the patient's skull was 996±167 HU, and that of the head phantom bone material

Table 1. Factors of the MRI scan of the patient-specific head phantom

MRI scan factors								
Slices	Voxel size	Bandwidth	Resolution	TE[1]	TE[2]	TE[3]	TE[4]	TR
77	1.4×1.4×2.0 mm	781 Hz/Px	256	36 ms	436 ms	835 ms	1,230 ms	2,000 ms

MRI, magnetic resonance imaging.

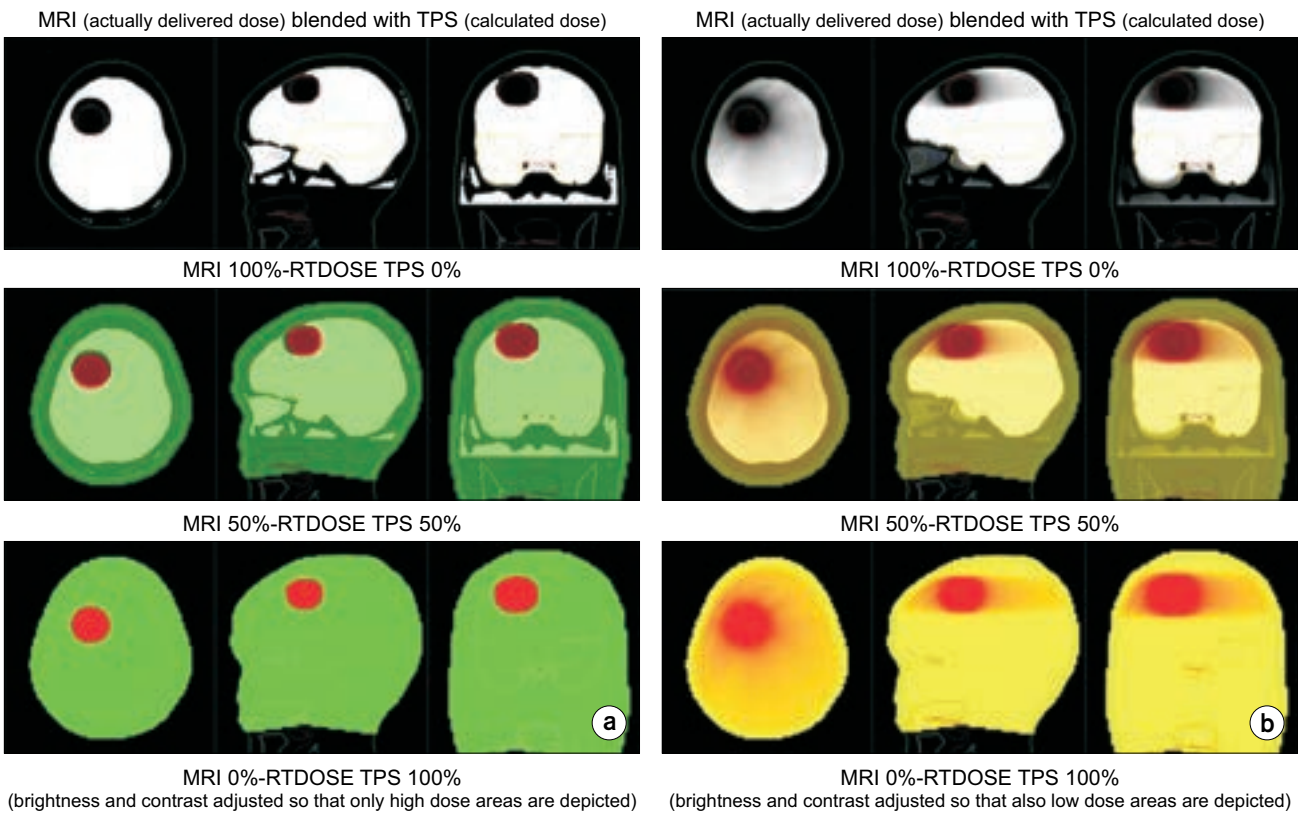

Fig. 4. (a) MRI image and treatment plan for high dose. (b) MRI image and treatment plan for low dose. MRI, magnetic resonance imaging; TPS, treatment planning system.

was 986±25 HU. This result covers the shortcomings of the resin powder that expresses high density, and it has been identified as the most challenging part of the existing ColorJet printing technology. Furthermore, the results indicate that resin powder with the added calcium has a density similar to that of human bones.

The electron density of the patient's brain was 58±15 HU, and that of the phantom was 45±17 HU. A 2 Gy radiation dose was irradiated through the treatment plan using the CT image of the patient. Then, it was scanned with MRI to compare and analyze the 3D distribution of the radiation dose prescribed in the treatment plan. The results are presented in Fig. 4, which shows the dose values calculated by the post-irradiation MRI images and TPS. The dose calculated through the image of the phantom and TPS is shown by adjusting the brightness by 100%, 50%, and 0%. Fig. 4a shows that only high dose areas are depicted with the brightness and contrast adjusted, and it indicates how this high-dose area—the dose calculated by the TPS—is delivered to the phantom. Fig. 4b shows that also low dose areas are depicted with the brightness and contrast adjusted, and it indicates the extent to which the dose calculated by TPS is delivered outside the central high-dose area. These two images suggest that the dose calculated by the treatment plan for the target to be treated is designed adequately to match the phantom manufactured.

2. Profile comparison

Fig. 5 shows the comparison results of the 3D distribution of the gel investigated by the treatment plan through the MRI scan and analysis results of the dose profile calculated through TPS. Fig. 5a and b present the analysis results of the dose profile in the *x*-axis and *y*-axis directions in the coronal plane of the phantom, and Fig. 5c and d present the analysis results of the dose profile in the *x*-axis and *y*-axis directions in the transverse plane of the phantom.

When comparing the 1D gamma index calculations for evaluating the agreement between the two data sets quantitatively, the passing criteria indicated a 2 mm distance to the agreement and a 5% dose difference. The dose profile results of the above evaluation are illustrated in Fig. 6. Based on the profile comparison, we confirmed that there was a shift between the dose distribution calculated from the TPS and the dose distribution irradiated to the phantom. Although the phantom was set up in the same position as the patient image in the treatment room using CBCT, only the error suggested after the first CBCT scan was applied, and a new scan was not conducted. This may have caused the setup to be inaccurate.

The 1D gamma index of the calculated dose and the absorbed dose matched the gamma passing criteria within 2 mm/2% when the graph was plotted for the absorbed dose from irradiating the gel phantom by 4.5 mm to the right. After correcting the error according to the position for the remaining directions, it was confirmed that the gamma passing rate was more than 95% in the gamma criteria of 2%/2 mm. Given the phantom setup and the low-dose exposure, it can be considered that the gel dosimetry conducted in this study will adequately match the dose from the TPS.

Discussion

Based on the CT images of brain cancer patients, we used

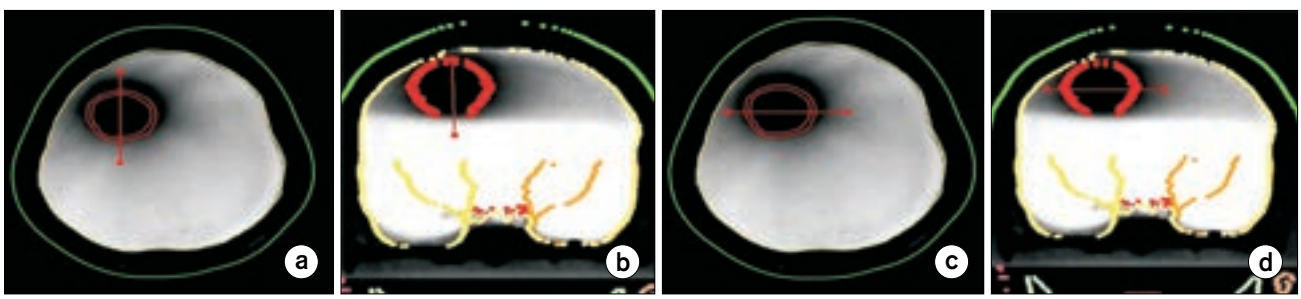

Fig. 5. (a) Dose profile in the *x*-axis direction of the coronal plane (T2 maps of the investigated phantom). The high-dose area is the dark area. (b) Dose profile in the *y*-direction of the coronal plane. (c) Dose profile in the *x*-direction of the transverse plane. (d) Dose profile in the *y*-axis direction of the transverse plane.

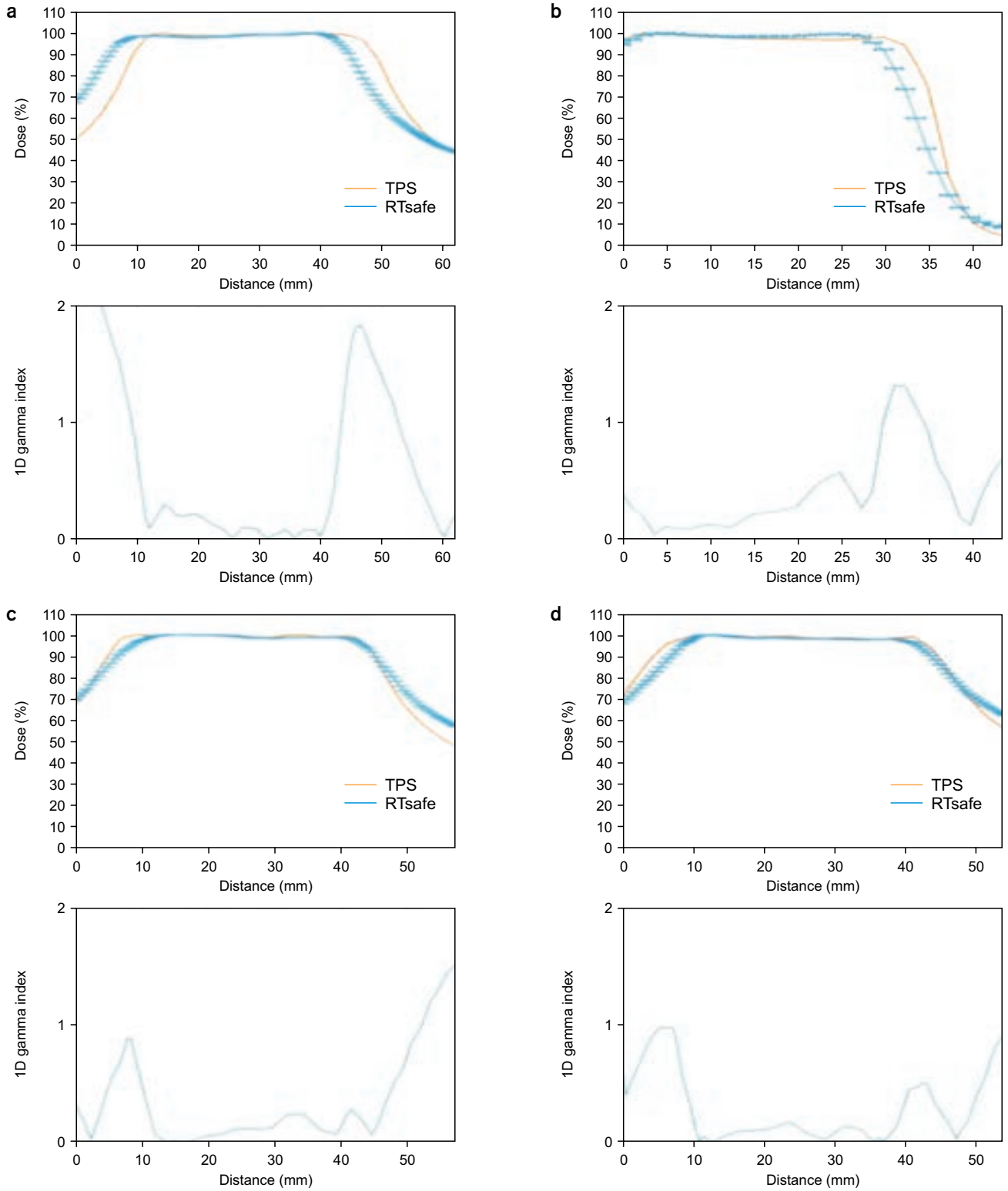

Fig. 6. Comparisons between one-dimensional (1D) profile and 1D gamma index values of the calculated (TPS) and measured doses: (a) *x*-axis direction of the coronal plane; (b) *y*-axis direction of the coronal plane; (c) *x*-axis direction of the transverse plane; (d) *y*-axis direction of the transverse plane. TPS, treatment planning system.

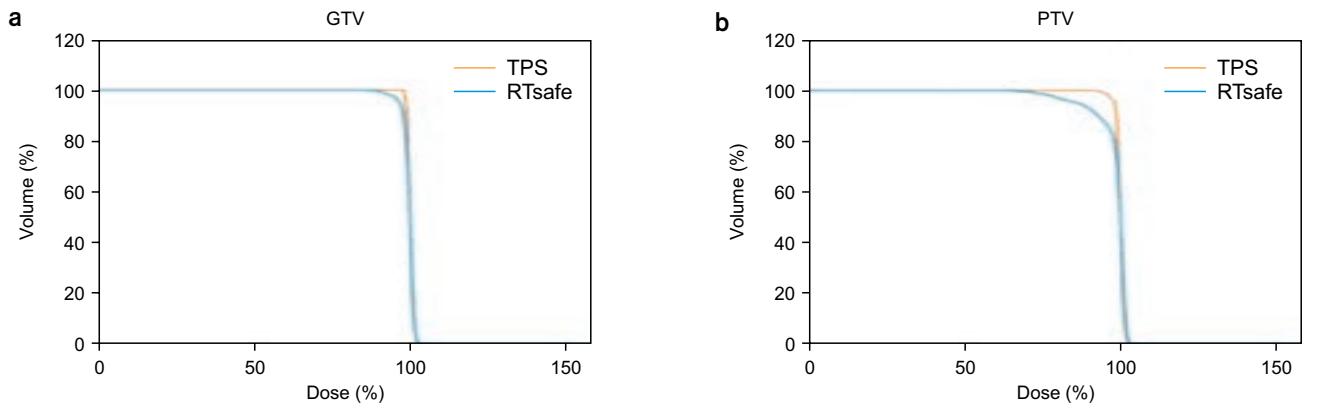

Fig. 7. Dose-volume histograms in (a) GTV and (b) PTV. GTV, gross tumor volume; PTV, planning target volume; TPS, treatment planning system.

3D printing technology to fabricate a patient-customized 3D phantom suitable for the density of each region, and performed 3D dose evaluation using a polymer gel inserted into the phantom. As suggested by Adam et al. [16], it was confirmed that the HU values of brain and bone were similar to those of the phantom produced in this study. Comparison of the HU values of the CT image of the patient and those of the phantom revealed that they were almost similar. These values were compared with the average HU values and their standard deviation obtained by designating three ROIs each to identify the homogeneity of the printed material. To analyze the three-dimensional dose distribution using the two-dimensional dose distribution, the dose volume histogram of PTV was compared. The results for the cumulative dose volume histogram of all PTVs are illustrated in Fig. 7 as a comparison between the planned relative dose distribution and the measured relative dose distribution. The difference between the calculated dose (TPS) and absorbed dose (RT-safe) in a gross tumor volume (GTV) can be observed from the results of the dose volume. As shown in Fig. 7, the high dose area of GTV matched well with the TPS results despite differences in the location of the scanned gel phantom. The difference between TPS and gel dosimetry for PTV showed more difference in the high dose area than the difference in GTV. The reason was analyzed as a difference due to the HU in the PTV area and the dose calculation algorithm. For comparing these results, the errors of the dose rate for the volumes of GTV and PTV are reduced when position correction is achieved for TPS and the measured gel.

Conclusions

In this study, a comparative analysis of a patient-customized phantom fabricated using 3D printing technology and a 3D dosimetry and TPS using a gel was performed. The 3D-printed head phantom has advantages such as dose comparison among patient's prescriptions, personalized quality assurance (QA), precision of phantom production, and various application possibilities. The accuracy of the patient treatment plan was verified through the DQA measurements conducted using pretreatment images and the results of the polymer gel dosimetry of an anthropomorphic phantom. The comparative analysis produced better results by validating the difficult-to-treat areas through QA using a customized 3D printing phantom. These results indicate that a customized phantom can be fabricated not only for the head but also for other body parts. It is expected that this study can be applied to the accurate patient specific dosimetry in high energy photon radiation therapy as well as particle radiation therapy.

Acknowledgements

This research was supported by the National Research Foundation of Korea (NRF) grant funded by the Korean government (Ministry of Sciences and ICT) (No. 2020M2D9A309417011).

Conflicts of Interest

The authors have nothing to disclose.

Availability of Data and Materials

All relevant data are within the paper and its Supporting Information files.

Author Contributions

Conceptualization: Yona Choi and Sang Hyoun Choi. Data curation: Yona Choi. Formal analysis: Yona Choi and Sang Hyoun Choi. Funding acquisition: Sang Hyoun Choi. Investigation: Yona Choi and Sang Hyoun Choi. Methodology: Kook Jin Chun and Geun Hee Kim. Project administration: Kum Bae Kim. Resources: Kook Jin Chun and Eun San Kim. Software: Ji-Ae Park and Geun Hee Kim. Supervision: Sang Hyoun Choi. Validation: Young Jae Jang. Visualization: Ji-Ae Park, Yona Choi, and Sang Hyoun Choi. Writing–original draft: Yona Choi. Writing–review & editing: Sang Hyoun Choi.

References

1. Ezzell GA, Galvin JM, Low D, Palta JR, Rosen I, Sharpe MB, et al. Guidance document on delivery, treatment planning, and clinical implementation of IMRT: report of the IMRT Subcommittee of the AAPM Radiation Therapy Committee. Med Phys. 2003;30:2089-2115.
2. Chin LS, Regine WF. Principles and practice of stereotactic radiosurgery. New York: Springer Science+Business Media; 2010.
3. Park HJ, Griffin RJ, Hui S, Levitt SH, Song CW. Radiation-induced vascular damage in tumors: implications of vascular damage in ablative hypofractionated radiotherapy (SBRT and SRS). Radiat Res. 2012;177:311-327.
4. Gigliotti MJ, Hasan S, Liang Y, Chen D, Fuhrer R, Wegner RE. A 10-year experience of linear accelerator-based stereotactic radiosurgery/radiotherapy (SRS/SRT) for paraganglioma: a single institution experience and review of the literature. J Radiosurg SBRT. 2018;5:183-190.
5. Kry SF, Molineu A, Kerns JR, Faught AM, Huang JY, Pulliam KB, et al. Institutional patient-specific IMRT QA does not predict unacceptable plan delivery. Int J Radiat Oncol Biol Phys. 2014;90:1195-1201.
6. Hillman Y, Kim J, Chetty I, Wen N. Refinement of MLC modeling improves commercial QA dosimetry system for SRS and SBRT patient-specific QA. Med Phys. 2018;45:1351-1359.
7. Kim JS, Park BR, Yoo J, Ha WH, Jang S, Jang WI, et al. Measurement uncertainty analysis of radiophotoluminescent glass dosimeter reader system based on GD-352M for estimation of protection quantity. Nucl Eng Technol. 2021. doi: 10.1016/j.net.2021.08.016.
8. Molazadeh M, Robatjazi M, Geraily G, Rezaeejam H, Zeinali A, Shirazi A. Three-dimensional IMRT QA of Monte Carlo and full scatter convolution algorithms based on 3D film dosimetry. Radiat Phys Chem. 2021;186:109528.
9. Choi JW, Choi JY, Kim BC, Joo KK. Feasibility study of a portable and fast spatial dosimeter using an alcohol-based liquid scintillator and a digital camera. J Korean Phys Soc. 2021;79:810-817.
10. Eidi T, Aghamiri SMR, Jaberi R, Baghani HR. On measuring the 3D dose distribution for notched and circular Ru-106 plaque shapes through Gafchromic film dosimetry approach. Radiat Phys Chem. 2022;190:109792.
11. Silveira MA, Pavoni JF, Baffa O. Three-dimensional quality assurance of IMRT prostate plans using gel dosimetry. Phys Med. 2017;34:1-6.
12. Lee M, Noh S, Yoon KJ, Lee SW, Yoon SM, Jung J, et al. Feasibility study of polymer gel dosimetry using a 3D printed phantom for liver cancer radiotherapy. J Korean Phys Soc. 2020;76:453-457.
13. Matrosic CK, Holmes S, Bednarz B, Culberson W. Evaluation of a clinical dose accumulation algorithm using deformable gel dosimetry. J Phys Conf Ser. 2019;1305:012002.
14. Baldock C, De Deene Y, Doran S, Ibbott G, Jirasek A, Lepage M, et al. Polymer gel dosimetry. Phys Med Biol. 2010;55:R1-R63.
15. Pérez P, Torres PR, Bruna A, Brunetto M, Aon E, Franco D, et al. Fricke gel xylenol orange dosimeter layers for stereotactic radiosurgery: a preliminary approach. Appl Radiat Isot. 2021;178:109936.
16. Hebb AO, Poliakov AV. Imaging of deep brain stimulation leads using extended Hounsfield unit CT. Stereotact Funct Neurosurg. 2009;87:155-160.